HiSST: International Conference on
High-Speed Vehicle Science Technology
26–29 November 2018, Moscow, Russia

Effect of Direct-Reverse Successive Changes of Equivalence Ratios on Transient Combustion in a Scramjet Combustor

Yue Huang [1], Wubingyi Shen[1],Zhenye Luan[1],Fei Xing[1],Yancheng You[1]

Abstract

The impact of successive increases and decreases of the equivalence ratios on unsteady characteristics in the transition of combustion modes of a hydrogen-fuelled dual-mode ramjet/scramjet combustor were simulated with DES and finite-rate chemistry model. The present studies were focused on the transient combustion features, the shock train structure and movement. The numerical results confirmed the main qualitative findings about the transition of combustion modes and wall pressure oscillation from the previous experiments. Transient interactions between shock train and multi-scale combustion for the successive decreases of the equivalence-ratios is distinguished from the inverse features of the successive increases of the equivalence-ratios. A detail flow analysis identified the factors contributing to transition of combustion modes for the varying of equivalence ratio are performed by the three dimensional flow visualization sequences.

Keywords: *Scramjet, Equivalence ratio, DES, Transition of combustion modes*

Nomenclature

Latin
Ma – Mach number
P – Pressure
T – Temperature
TFI – Takeno Flame Index
Y – Mass fraction
Greek
φ – Equivalence ratio
ρ – Density
Subscripts
1 – Maximum disturbance point
2 – Minimum disturbance point

1. Introduction

Dual-mode scramjet combustor has been considered as one of the most important component for the hypersonic propulsion systems. The key advantage of the dual-mode scramjet combustor, as compared to conventional rocket engines, is without carrying oxidant. However, the dual-mode scramjet engine requires a booster to facilitate the transition from a low Mach number take-off to a supersonic cruise. For this reason, the flight-test experiments of the dual-mode scramjet combustor are costly. Therefore, most experimental data of the dual-mode scramjet combustor was obtained in the ground test, which also brought about the accuracy problem. To further complement the data and reduce the cost, numerical simulations have been used to gain further physical insight in the physics of the transition of combustion modes.

Traditionally, two different experimental approaches have been followed to facilitate the transition of combustion modes: Changes of the incoming flow conditions [1] and the effective fuel equivalence ratio. The fuel injection pressure, [2] and the injector position, [3] could change the effective fuel equivalence ratio. The HyShot II experiment conducted by the University of Queensland [4] is one of the most famous experiments. Hydrogen supersonic combustion data was successfully collected during approximately three seconds, in an altitude range from 35 km to 23km. In order to make better use of flight test data, the ground test of HyShot II scramjet has been performed in the HEG tunnel of the German Aerospace Centre,[5].

[1] *School of Aerospace Engineering, Xiamen University, Xiamen, 361005, China*

In the previous work, researchers investigated the transient combustion features, the shock train structure and movement by numerical simulations. Baurle et al [6] analyse the dual-mode hydrocarbon scramjet operation at Mach 4 to 6.5, and they find that even if the combustor mixing efficiency at Mach 6 is lower than that of Mach 4, the combustion efficiency of both is equal due primarily to the shock-induced flow distortion and lager residence time. YU et al [7] interprets the characteristic of combustion mode transition based on the cusp topological model in singular theories, and observe the bifurcation characteristic in combustion mode transition. Tekin et al [8] conducted non-adiabatic flamelet combustion model for resolving finite rate chemistry effects on the dual-mode scramjet combustor. Based on the experiment data of the HyShot II scramjet, many researchers have studied the catastrophe, hysteresis and bifurcation from the aspects of heat released characteristics, turbulent combustion model, shock train propagation and initial pressure distribution, [9-15].

Many numerical simulations and experiments for the dual-mode scramjet combustor have been completed. However, there are still many problems left to be resolved. For the experiments, there are no new measurement methods for accurate analysis of the mixing and heat release characteristics, which cause hysteresis. The mode transitions were investigated using Reynolds-Averaged Simulation lack of the high-dimensional numerical simulation. In this paper, the numerical simulation of the HyShot II 2D model is used to verify the combustion mode by the pressure ratio of maximum and minimum disturbance point. The Detached-Eddy Simulation is used to investigate the hysteresis during successive increases and decreases of the equivalence ratios. The CFD++ code was used for the present study. It has been found that the shock train in the isolator increases residence time for the process of liquid fuel evaporating and mixing. A slight increase/decrease in the equivalence ratio affects the chemical reaction products.

2. Computation Setup

2.1. Governing Equations and Numerical Methods

Compressible perfect gas Naiver-Stokes equations, in three-dimensional Cartesian coordinates are selected. The turbulent combustion model adopts thickened flame model. Thickened flame model is based on phenomenological formulation of laminar flame speed for premixed flames. At steady state the laminar flame structure comprises a preheat zone and a thin reaction zone. Almost all of the chemical activity is confined to the thin zone. The preheat zone is thicker than the reaction zone. Heat flux balance between the steady reaction zone and the preheat zone leads the following equations. For these simulations, the turbulence model is Shear Stress Transport turbulence model. The difference format is TVD-HLLC (Total Variation Diminishing), the time integral method is implicit Euler method. The chemical reaction mechanism is hydrogen/oxygen 7 component 7 step element reaction, [16].

2.2. Geometry, Computational Domain and Operation Conditions

The flow field inside the HyShot combustion chamber is simulated using a three-dimensional computational domain. Three-dimensional model is composed of a wedge-shaped intake ramp, a rectilinear combustion chamber and a single expansion exhaust nozzle. Computational domain and boundary conditions are defined in Fig. 1. The inlet condition of the combustion base on the inlet RANS calculation data. The walls are the isothermal walls with the temperature of 300K. The injector is specified as the total pressure and the total temperature. The outlet condition is the supersonic outlet. Air stream boundary conditions are derived from the RANS data, [17] with the Prandtl number of 0.89, Schmidt number of 0.7. Time step is 5×10^{-7}s. HyShot II 2D model case is set to the same condition expect the time step of 10^{-6}s.

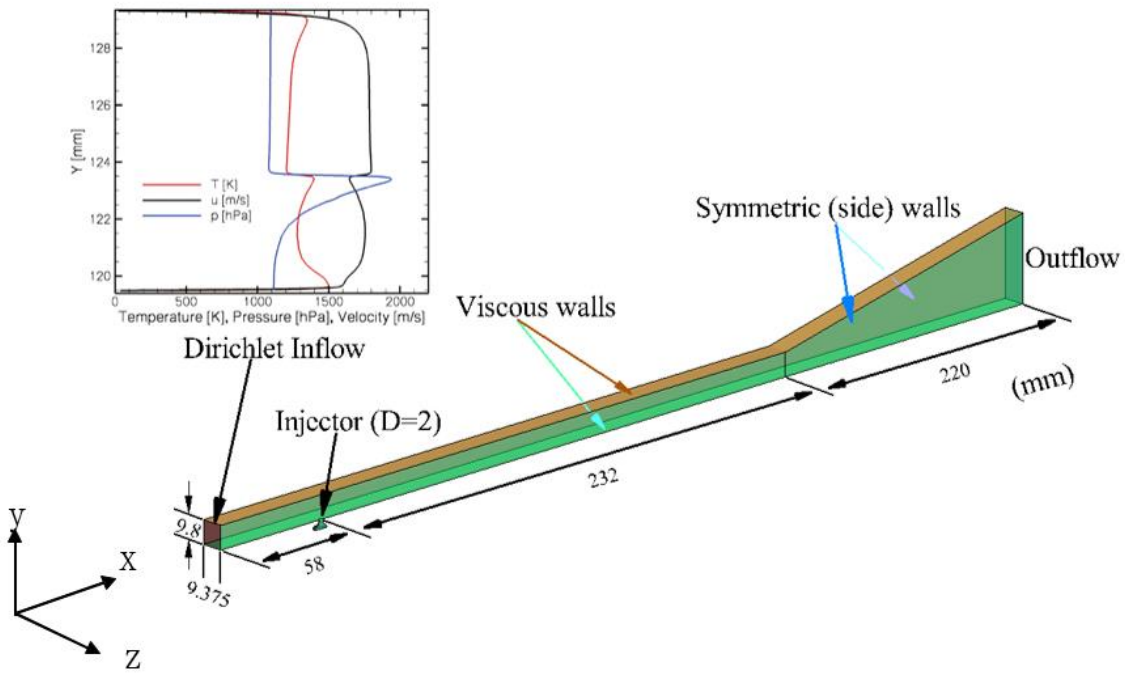

Fig 1 HyShot II boundary conditions

Commercial grid generator ICEM is used to generate multi-block structured grids for the computational domain. The detail of 3D grid topology is shown in Fig. 2. In the wall normal direction, the first layer thickness is scaled to 3×10^{-6}m. In the region of the injector, where shock train and shear layers exist, the number of the grid increases. Structured grid is Y+=1-5. The total number of grids is 12 million.

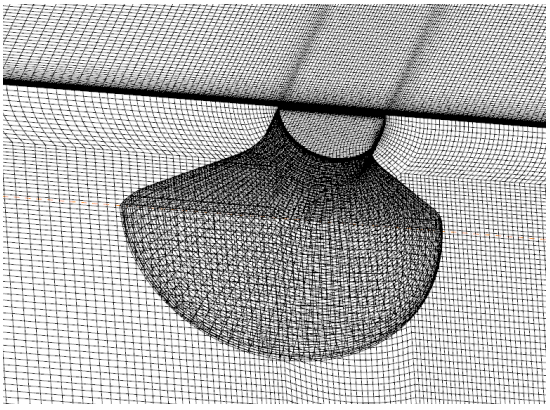

Fig 2 HyShot II grid

2.3. Numerical Methods Validation

This validation aims to evaluate whether the skeletal reaction mechanism can meet the demand and the numerical method can predict the flow field. The HyShot II experiments at HEG in DLR are used to provide data for the validation study. Five kinds of hydrogen/oxygen skeletal reaction mechanisms are listed in Fig. 3, [22-25]. As shown by the comparison of the laminar flame propagation velocity under different equivalence ratios, 7 components 7steps mechanism can indicate all most of chemical activity in this paper, [25].

Fig. 4 shows the pressure distribution as well as heat flux on the injector sidewall, and it is clearly obvious that the numerical results show very good agreement with the experiment data. It can obtain good shock train and combustion flow field structure. This may imply that the numerical approach employed is with confident to conduct the following investigation.

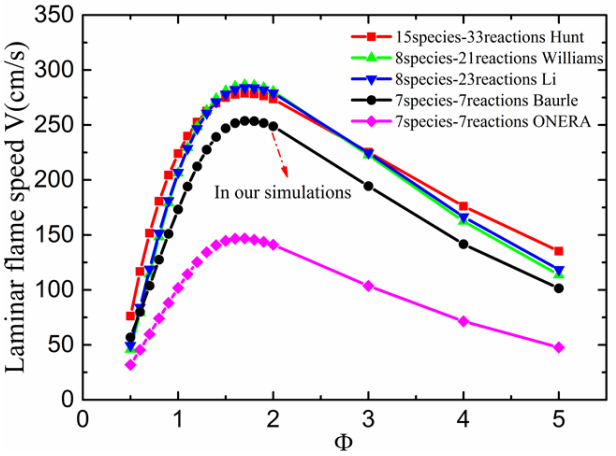

Fig 3 Comparison of simulated reaction mechanism of hydrogen in common

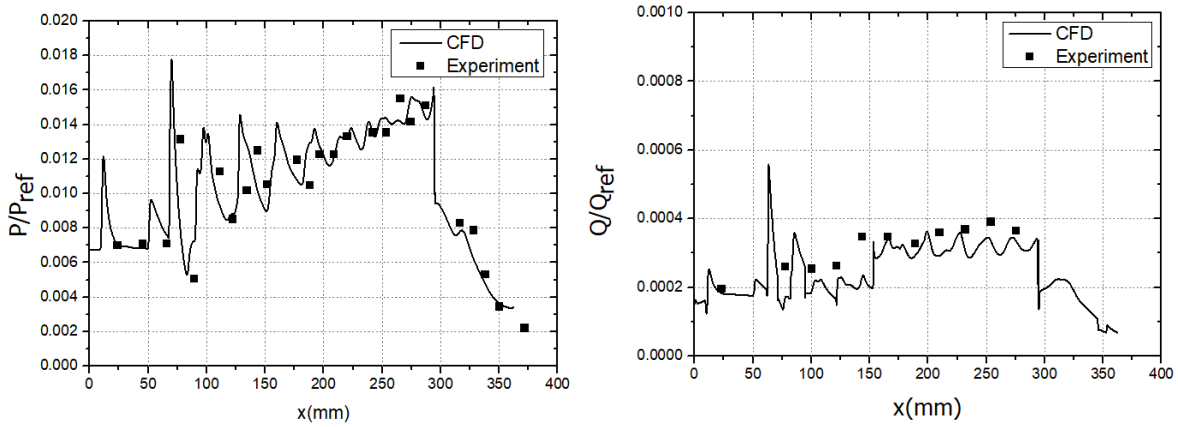

Fig 4 Comparison of numerical simulation results with experiment data φ=0.295（left-Pressure，right-Heat flux）

3. Results and Discussion

3.1. 2D Model

When the equivalence ratio successively increases, the pressure distributions of the upper and lower wall are shown in Fig. 5. As the equivalence ration increases, the amount of heat released and the pressure in the combustion chamber increase. When the equivalence ratio is 0.361, the boundary layer of the isolator is separated, and the pressure propagates upstream along the boundary layer, resulting in the shock train in the isolator. What can be clearly seen in Fig. 5 is the phenomenal growth of the pressure of the lower and upper wall when the equivalence ration is 0.474. The mass-weighted average Mach number in the combustion chamber is 1.09. The maximum disturbance point is x=0.0384m. In the process of changing the equivalence ratio from 0.539 to 0.903, it could be observed that the pressure distribution of the upper and lower wall of the HyShot II combustion chamber remains unchanged and combustion mode transforms into the ramjet combustion mode.

When the equivalence ratio successive decreases, the pressure distributions of the upper and lower wall are shown in Fig. 6. As the equivalence ratio decreases, the combustion chamber pressure decreases, the pressure of the upper and lower wall decreases, and the boundary layer separation phenomenon of the isolator and the shock wave generated by the action of the upstream isolator gradually disappear. Fig. 6 reveals that there has been a sharp drop of pressure of the upper and lower wall in the equivalent ratio of 0.539. The mass-weighted average Mach number in the combustion chamber is 1.03. When the equivalence ratio is 0.34, the shock train in the isolator disappears. In the process of changing the equivalence ratio from 0.474 to 0.122, what can be clearly seen is that the

pressure distribution of the upper and lower wall of the HyShot II combustion chamber remains unchanged and the combustion mode transforms into the scramjet combustion mode.

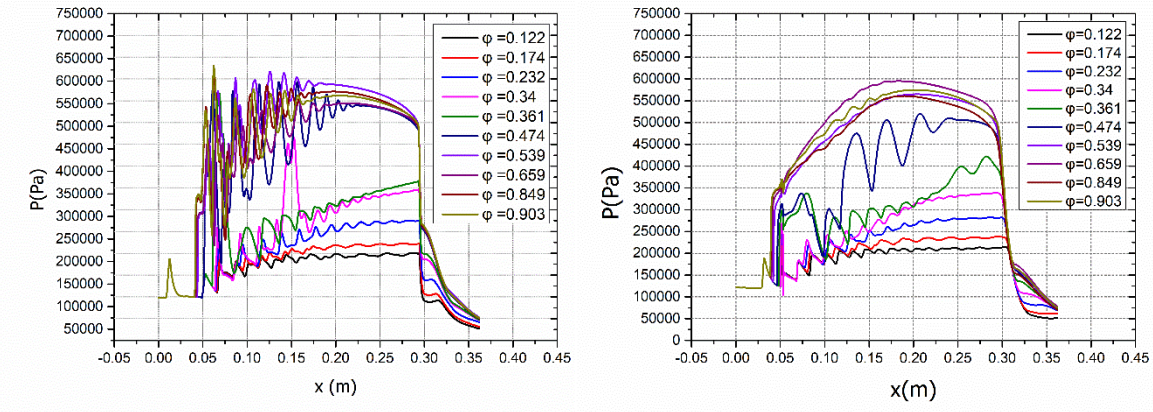

Fig 5 Equivalent ratio increases wall pressure distributions（left-upper wall，right-lower wall）

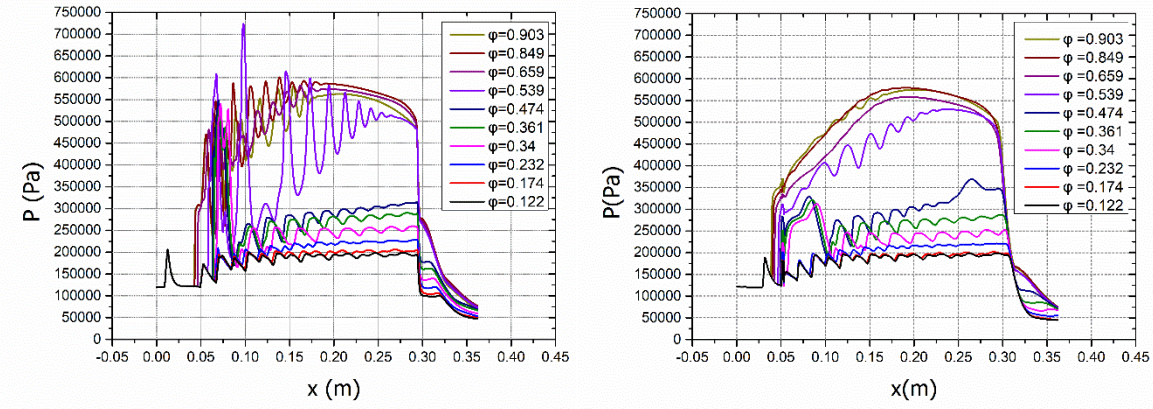

Fig 6 Equivalent ratio decreases wall pressure distributions（left-upper wall，right-lower wall）

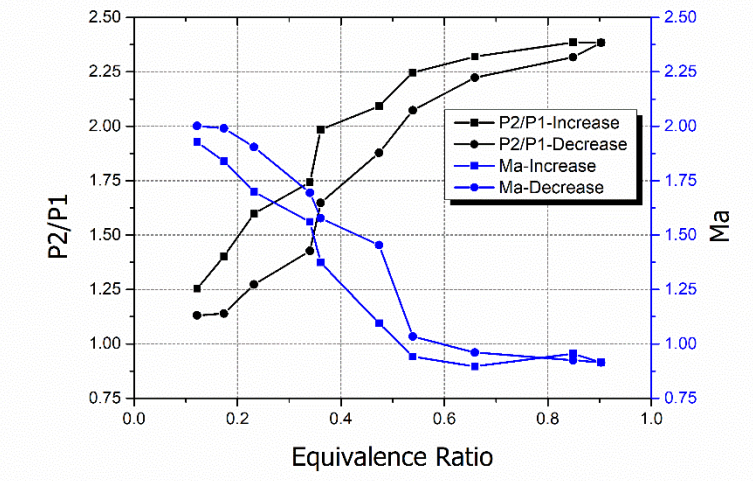

Fig 7 Maximum disturbance point and minimum disturbance point Pressure ratio and combustion chamber mass average Mach number（Black font is Maximum disturbance point and minimum disturbance point Pressure ratio；Blue font is combustion chamber mass average Mach number）

The pressure of the maximum disturbance point (x=0.0384) in the lower wall is P_1 and the pressure of the minimum disturbance point(x=0.051m) in the lower wall is P_2. As shown in Fig. 7, the dimensionless treatment is performed using P_1 and P_2. Taken together, these results suggest that when $P_2/P_1<2$, the HyShot II combustion chamber would operate on the scramjet combustion mode. When $P_2/P_1\geqslant 2$, the HyShot II combustion chamber would operate on the ramjet combustion mode. In summary, when the

equivalent ratio increases, φ=0.474 is the mode transition point. When the equivalent ratio decreases, φ=0.539 is the mode transition point.

3.2. 3D Model

Fig. 8 presents distributions, from top to bottom, temperature, T, pressure, P, Mach number, Ma, density gradient, $|\nabla\rho|$, mixture fraction, Z, Takeno Flame Index, TFI. In order to identify the combustion mode, TFI is adopted for identification of premixed or non-premixed mode. TFI greater than zero indicates the premixed flame while TFI less than zero indicates the non-premixed flame. Initial observations suggest that the pressure distribution is dominated by a shock-system. It could be found that the TFI is less than zero where the combustion occurs in the downstream of the injector, which suggests that the flame is dominated by non-premixed mode especially in the mixing layer near the lower wall. The pressure and temperature are significantly increased at the rear of the premixed flame in the combustion chamber. The bow shock compression increases the temperature upstream recirculation zone and windward side of injector exit, which promote combustion and the flame stabilization. The large amount of heat released in this area causes the temperature and pressure to increase rapidly. Combustion also take place near the bottom wall downstream the location x=0.190m, which is due to the continuous compression heating to the mixture by reflected oblique shock.

In the process of the increased equivalence ratio, it could be observed that it exhibits a high temperature region A at x=0.051m, and the high temperature region B that continues to expand in the middle of the combustion chamber at x=0.092m at 7.25ms. Correspondingly, temperature distribution of the combustion chamber shown in Fig. 9 also changes drastically. The observations based on Fig. 9 suggest that there may be a link between chemical reaction product and temperature distribution. Temperature rises to a high point and peaks in Y_{H_2O} =0.225 in Fig. 10 (a) and in Z=0.2 (b). The data reported here appear to support the assumption that chemical reaction product have impact on the temperature distribution. Fig. 10 also presents temperature distributions, from top to bottom, the middle part, the part near the lower wall and the part near the upper wall.

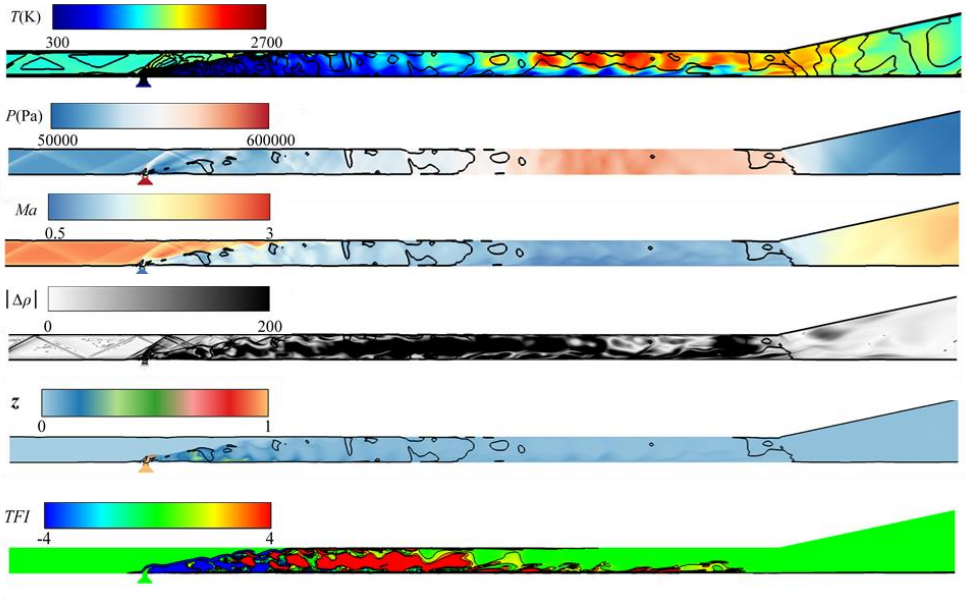

Fig 8 Combustion flow field simulation results (φ=0.415, injector sidewall)

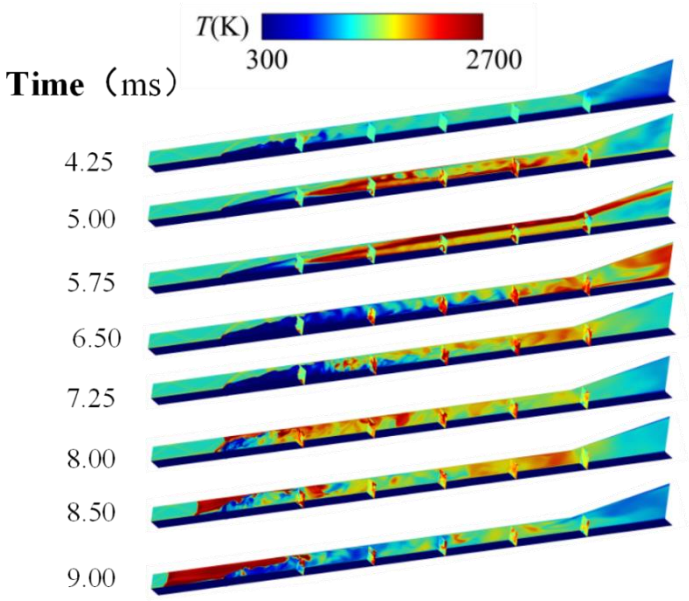

Fig 9 Variable equivalence ratio temperature distribution of Hyshot II combustor (φ=0.539)

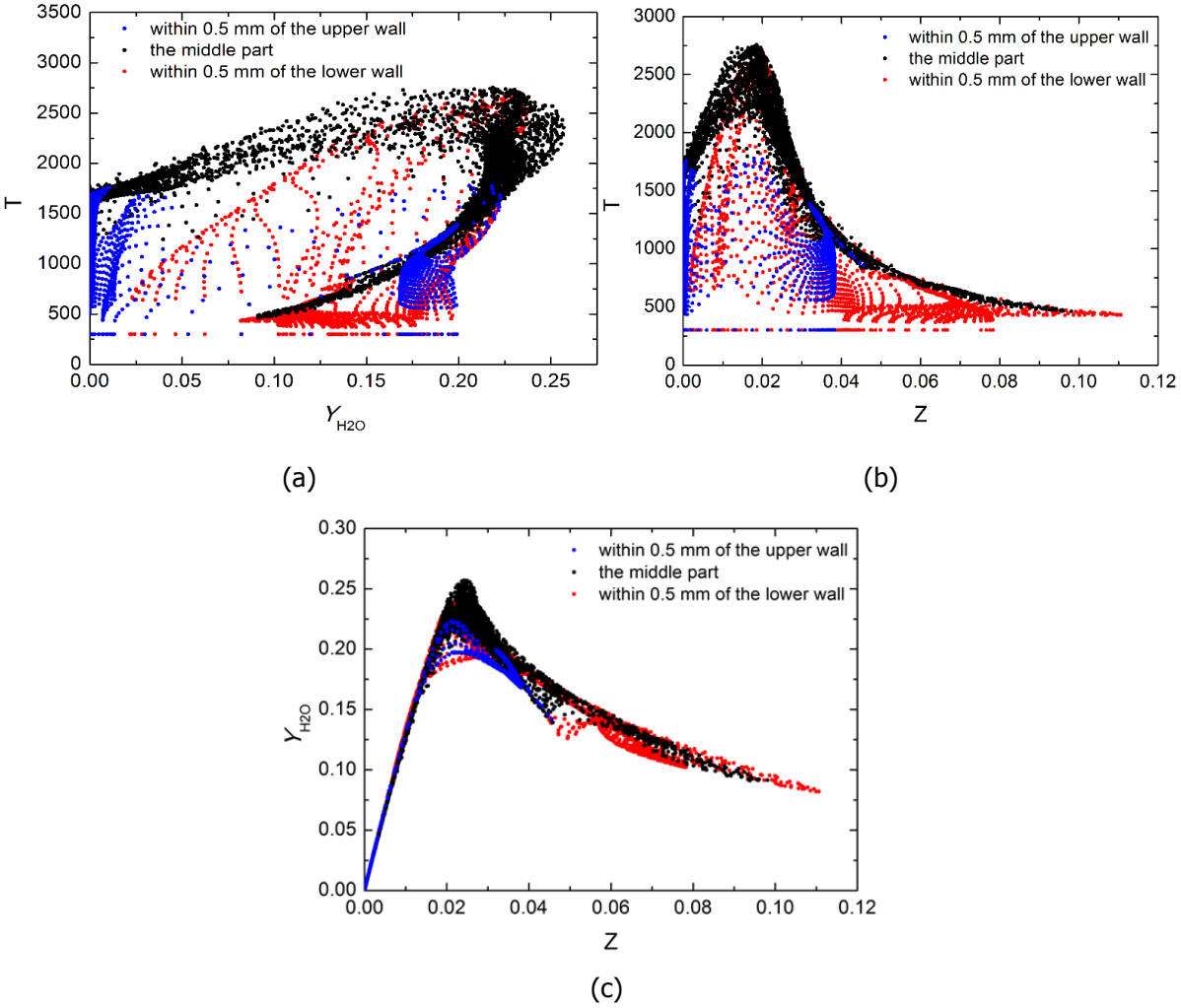

Fig 10 Scatter plot（a-Y_{H2O}-T，b-Z-T,c-Z-Y_{H2O}）

The scatter plots of different modes of the HyShot II combustion are listed in Fig. 11 and Fig. 12. In the scramjet combustion mode, the temperature reaches the peak at the Y_{H_2O} =0.225, where hydrogen

injected can be completely burned. By comparison, it can be obtained that in the ramjet combustion mode, although the equivalence ratio increases, but it generates less free radicals and the combustion efficiency is lower than that in the scramjet combustion mode. In the ramjet combustion mode, the mass fraction of OH is higher, and the temperature and the mass fraction of OH, H_2O rise to the peak at the same time. According to Fig. 8, Fig. 11, Fig. 12, a small amount of hydrogen is separated from the shear flow around injection. Simultaneously, this part of the hydrogen compressed by the bow wave results in the temperature rise and spontaneous combustion. The free radicals generated by combustion and H_2O form the thin-wall layer, and the interaction between the shock wave and the thin-wall layer further promotes the process.

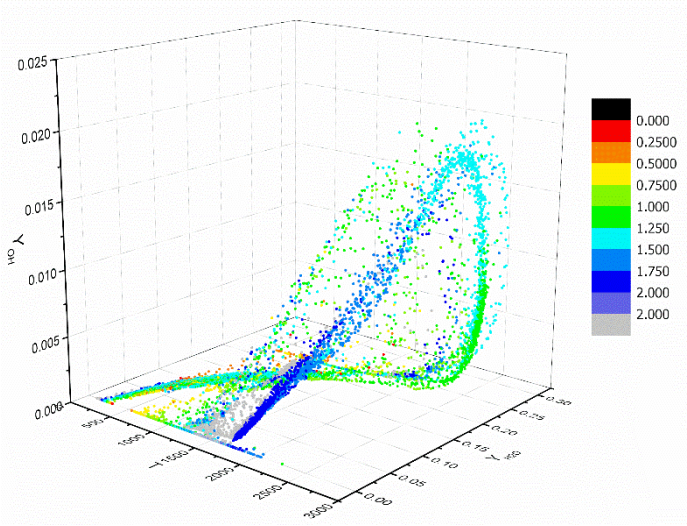

Fig 11 Scatter diagram scramjet combustion（X-T,Y-Y_{H2O}, Z-Y_{OH}）

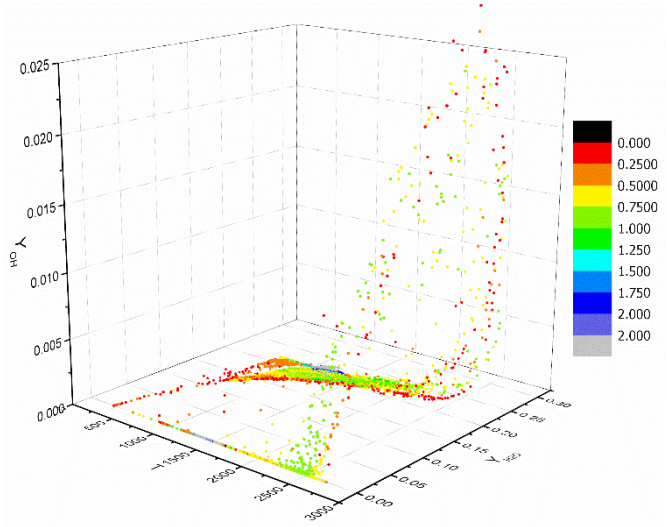

Fig 12 Scatter diagram ramjet combustion （X-T,Y-Y_{H2O}, Z-Y_{OH}）

4. Conclusion

In this paper, the numerical results confirmed the main qualitative findings about the transition of combustion modes and wall pressure oscillation from the previous experiments. Transient interactions between shock train and multi-scale combustion for the successive decreases of the equivalence-ratios is distinguished from the inverse features of the successive increases of the equivalence-ratios. The mode transition can be judged based on the P_2/ P_1. The Y_{OH} influents the performance of dual-mode combustion chamber. The free OH radicals generated by combustion further promotes the combustion.

References

1. Sullins, G.A.: A Demonstration of Mode Transition in a Scramjet Combustor. AIAA J, 9, 515-520 (1991).
2. Denis, S. R., Brand Stetter, A., Kau, H. P.: Experimental Study on Transition between Ramjet and Scramjet Modes in a Dual-Mode Combustor. AIAA J., (2013).
3. Kanda, T., Chinzei, N., Kudo, K., et al.: Dual-Mode Operations in a Scramjet Combustor. Journal of Propulsion & Power, 20(4):760-763 (2012) .
4. Smart, M. K., Hass, N. E., Paull, A.: Flight Data Analysis of the HyShot 2 Scramjet Flight Experiment. AIAA J, 44(10):2366-2375 (2005).
5. Gardner, A. D., Hannemann, K., Paull, A., et al.: Ground testing of the HyShot Supersonic Combustion Flight Experiment in HEG. International Symposium on Shock Waves Volume,329-334 (2004).
6. Baurle, R. A., Eklund, D. R.: Analysis of Dual-Mode Hydrocarbon Scramjet Operation at Mach 4-6.5. J. Propul. Power, 18(5):990-1002 (2002).
7. Daren, Y. U.: Catastrophe, Hysteresis and Bifurcation of Mode Transition in Scramjet Engines and its Model. Sci. China-Phys. Mech. Astron., 52(6):1543-1550 (2009).
8. Aksu, T., Uslu, S.: Large-Eddy Simulation of a Dual-Mode Scramjet Combustor Using non-Adiabatic Flamelet Modeling. AIAA, (2017).
9. F, Xing, Y. Zhu., Y. Huang., et al: Numerical Analysis of HyShot Scramjet Model with Different Throat Heights. AIAA, (2017).
10. C. P. Chen., D. C. Liu.: Numerical Investigation of Supersonic Combustion of the HyShot Ⅱ in the Shock Tunnel. Journal of Aeronautics Astronautics & Aviation, 43(2):119-127 (2011).
11. Nordin-Bates K., Fureby C., Karl S., et al: Understanding Scramjet Combustion using LES of the HyShot II combustor. Proc. Combust. Inst., 2015-3615 (2015).
12. Defoort, S., Ferrier, M., Viguier P., et al.: HyShot-II Experiments in the Onera F4 Hotshot Windtunnel: Lessons learnt from post-run Analysis and Comparison with existing data. AIAA, (2015).
13. Yentsch R. J., Gaitonde D. V.: Unsteady Three-Dimensional Phenomena in Mode-Transition Simulations of the HIFiRE-2 Scramjet Flow Path. AIAA. (2013).
14. Sebastian Karl, Stuart Laurence, et al.: CFD Analysis of Unsteady Combustion Phenomena in the HyShot-II Scramjet Configuration. AIAA, (2012).
15. Nordinbates, K., Fureby, C.: Understanding Scramjet Combustion using LES of the HyShot II Combustor: Stable Combustion and Incipient Thermal Choking. AIAA, (2013).
16. Baurle, R.A., Girimaji, S.S.: Assumed PDF Turbulence-Chemistry Closure with Temperature-Composition Correlations. Combust. Flame, 131–148(2003).
17. Karl, S.: Numerical Investigation of a Generic Scramjet Configuration. PhD thesis (2013).
18. Hunt, D. C.: Supersonic Combustion in Inlet-fuelled Busemann-Like Axisymmetric Scramjet Flow Paths. PhD thesis, (2014).
19. Priyank Saxena, Forman A. Williams.: Testing a Small Detailed Chemical-Kinetic Mechanism for the Combustion of Hydrogen and Carbon Monoxide. Combust. Flame, 145, 316–323 (2006).
20. J. Li, Z. Zhao, Kazakov A, et al：A Comprehensive Kinetic Mechanism for CO, CH2O, and C3OH Combustion. Int. J. Chem. Kinet, 39(3):109-136（2010）.